

Analytical Methods

Accepted Manuscript



This is an *Accepted Manuscript*, which has been through the Royal Society of Chemistry peer review process and has been accepted for publication.

Accepted Manuscripts are published online shortly after acceptance, before technical editing, formatting and proof reading. Using this free service, authors can make their results available to the community, in citable form, before we publish the edited article. We will replace this *Accepted Manuscript* with the edited and formatted *Advance Article* as soon as it is available.

You can find more information about *Accepted Manuscripts* in the [Information for Authors](#).

Please note that technical editing may introduce minor changes to the text and/or graphics, which may alter content. The journal's standard [Terms & Conditions](#) and the [Ethical guidelines](#) still apply. In no event shall the Royal Society of Chemistry be held responsible for any errors or omissions in this *Accepted Manuscript* or any consequences arising from the use of any information it contains.



Analytical Methods

ARTICLE

Fabrication and Electrochemical Characterization of Dopamine Sensing Electrode Based on Modified Graphene Nanosheets

M. Bagherzadeh,^{*a} S.A. Mozaffari^b and M. Momeni^bReceived 00th January 20xx,
Accepted 00th January 20xx

DOI: 10.1039/x0xx00000x

www.rsc.org/

Herein, by combining the unique electronic properties of graphene nanosheets (GNS) and Pt nanoparticles with the excellent properties of poly aniline (PANI), a nanocomposite of GNS/Pt/PANI was prepared and characterized by physical and chemical methods. Prepared GNS/Pt/PANI nanocomposite was applied for modification of a glassy carbon electrode (GCE) and served for detection of DA. The performance of the prepared GNS/Pt/PANI nanostructure was compared with the other similar nanostructure like GNS/PANI, CNT/Pt/PANI, GNS/CNT/PANI, and GNS/CNT/Pt/PANI. The results exhibited more favorable electron transfer kinetics and electrocatalytic activity towards the oxidation of DA respect to the AA. In optimized experimental and instrumental conditions, two linear calibration curves from 2.0 to 10 and 40 to 400 μM DA with slopes of 1.53 and 0.35 $\mu\text{A}/\mu\text{M}$, respectively, $r=0.99$, and the detection limit of 0.6 μM DA was observed at pH 7.4 for GNS/Pt/PANI/GCE. Prepared sensor showed good sensitivity, repeatability, and reproducibility in this work.

1. Introduction

Dopamine (DA) is one of the most important natural catecholamine neurotransmitters in the mammalian brain, playing a significant role in the function of the central nervous, renal and hormonal systems. The abnormal levels of DA may result in several diseases and neurological disorders such as schizophrenia, Parkinson's and Alzheimer's diseases [1]. Various analytical techniques including capillary electrophoresis (CE), high performance liquid chromatography (HPLC), flow injection analysis and spectrophotometry have been used to determine DA [2-5]. Since neurotransmitters such as DA are electroactive, electrochemical methods appear to be suitable for their quantitative determination [6,7]. However, at regular solid electrodes, DA and its coexisting species ascorbic acid (AA) have an overlapping sensitive redox reaction based on the voltammetric response, resulting in rather poor selectivity and sensitivity [8]. Thus, it is desirable for diagnostic applications to develop simple and rapid method for the determination of DA with high selectivity and sensitivity.

Nowadays new nanomaterials were served in construction of electrodes for electrochemical sensing [9-14]. One of the most important new materials is graphene. Graphene, a two-dimensional sheet of carbon atoms bonded through sp^2 hybridization, has been considered as a "rising-star" carbon material. Graphene has been intensively researched because of its remarkable properties, such as large surface area, high

electrical and thermal conductivities, high mechanical strength and potentially low manufacturing cost [15]. Compared to the other carbon allotropes, graphene has a higher surface area, more excellent electrical conductivity and electron mobility at room temperature [16,17]. The high surface area is helpful in increasing the surface loading of the target molecules on the surface. The excellent conductivity and small band gap are favorable for conducting electrons to/from biomolecules [18-20].

Conducting polymers, such as polyaniline (PANI), polypyrrole (PPY), poly(3,4-ethylenedioxythiophene) (PEDOT) and their composites, have also been widely used in electrode surface modifications [21-23]. Of these conducting polymers, PANI has attracted much attention due to its unique and controllable chemical and electrical properties, easily synthesis, biocompatibility, high electrochemical and environmental stabilities [24]. PANI finds important applications in solid electrolyte capacitors, energy storage systems, electrochromic devices, and electrochemical sensors. PANI also finds an important role in separation science, where it is used as ion-exchange membranes, supported films, and surface layers for applications ranging from gas separation to electrodialysis. In most of the above-mentioned studies, electronic properties of PANI have been explored, whereas only a few applications are based on its ion-exchange properties [25].

In the present work, by combining the unique electronic properties of graphene nanosheets (GNS) and Pt nanoparticles with the above-mentioned excellent properties of PANI, a nanocomposite of GNS/Pt/PANI was prepared and characterized by physical and chemical methods. Prepared GNS/Pt/PANI nanocomposite was applied for modification of a glassy carbon electrode (GCE) and served for detection of DA. The other same nanocomposites like GNS/PANI, CNT/Pt/PANI,

^a Material Research School, NSTRI, 81465-1589, Isfahan, I.R. IRAN.^b Thin Layer and Nanotechnology Laboratory, Department of Chemical Technology, Iranian Research Organization for Science and Technology (IROST), P.O. Box 33535-111, Tehran, Iran.^{*}Corresponding author. E-mail address: mjmo123@yahoo.com (Dr. M. Bagherzadeh).

GNS/CNT/PANI, and GNS/CNT/Pt/PANI were prepared and their performance on the detection of DA were compared with GNS/Pt/PANI. Among them, the GNS/Pt/PANI/GCE electrode exhibited favorable electron transfer kinetics and electrocatalytic activity towards the oxidation of DA in comparison to AA. Selective determination of DA was performed in the presence excess amount of AA at the GNS/Pt/PANI/GCE electrode, and DA was detected with good sensitivity and selectivity.

2. Experimental

2.1. Chemicals

Dopamine, ascorbic acid, glucose, polyaniline, platinum, graphite powder (spectrum grade, average particle size of 4 μm) and other materials used in this work were of analytical grade (Merck® or Aldrich®) and used without further purification. Phosphate buffer saline solutions (PBS) in the pH range of 2.0 to 8.5 were prepared using Smally's method [26]. The initial pH was ca. 2.1 for 0.1 M NaClO_4 + 0.01 M H_3PO_4 . All aqueous solutions were prepared with ultrapure water (>18 M Ω) from a Milli-Q Plus system (Millipore).

2.2. Synthesis of Graphene Oxide (GO) and Graphene Nanosheets (GNS)

GO was synthesized from natural graphite powder according to a modified Hummers method [27]. Chemically converted GNS are prepared by reduction of GO [28].

2.3. Instruments

The structure of the prepared GNS/Pt/PANI nanocomposite was studied by a low angle X-ray diffractometer (XRD, PHILIPS PW 1800 model) using $\text{CuK}\alpha$ radiation ($\lambda=1.5406 \text{ \AA}$). Morphology and elemental analysis of the samples determined by scanning electron microscope (SEM) (Philips XL-30). Furthermore, the quantitative analysis of energy-dispersive X-ray spectroscopy (EDX) was performed to identify chemical composition of nanocomposite layer. The shape and size of nanocomposites were identified by transmission electron microscopy (TEM) using a Philips-EM-2085 transmission electron microscope with an accelerating voltage of 100.0 kV.

All electrochemical measurements including cyclic voltammetry (CV), differential pulse voltammetry (DPV) were carried out using Metrohm 797VA (Herisau, Switzerland). The CV experiments were carried out in a quiescent solution at 100 mVs^{-1} in an electrochemical cell with 0.1 M PBS (pH 7.4). A three-electrode conventional cell including the modified GCE as working electrode, a large surface area Pt plate (99.99%) as the auxiliary electrode, and a Ag/AgCl (saturated KCl) electrode as the reference, was used for electrochemical measurements. All experiments were carried out at room temperature.

2.4. Fabrication of the modified electrode

The glassy carbon electrode (3 mm diameter) was polished to a mirror-like surface with 1.0 and 0.3 μm alumina slurry and washed thoroughly with ultrapure water. Afterwards, 8 μL of 10 mg mL^{-1} GNS/Pt/PANI nanocomposite suspension, after ultrasonication in distilled ethanol to form a homogenous dispersion, was dropped to fully cover the surface of the polished electrode and dried at room temperature for 90 min. The GNS/Pt/PANI/GCE electrode was put in to 0.1 M PBS (pH 5.0) for applying 5 cycles of cyclic voltammograms in a potential range from -0.5 to 1 V.

Same procedure was applied for modification of GCE by other modifiers i.e. CNT/PANI, GNS/PANI, CNT/Pt/PANI, GNS/CNT/PANI, and GNS/CNT/Pt/PANI in addition to GNS, PANI and CNT.

3. Results and discussion

3.1. Characterization of GNS/Pt/PANI nanocomposite

The XRD pattern of the GNS/Pt/PANI is shown in Fig. 1A. The GNS/Pt/PANI exhibited Bragg diffractions corresponding to the GNS [6]. The appearance of a wide peak around 2θ of 26° is corresponded to the characteristic (002) of GNS. The TEM was carried out for studying the size of GNS/Pt/PANI nanocomposite. The TEM images indicated the presence of Pt nanoparticles covered with PANI that dispersed on a GNS with an average size of 40 nm (Fig. 1B).

The morphologies and elemental composition of GNS/Pt/PANI nanocomposite was also analyzed by the SEM and EDX analysis, respectively (Fig. 1C and D). As can be seen from the SEM image (Fig. 1C), morphology of bulk GNS/Pt/PANI nanocomposite is regular and their distribution is uniform. In the EDX spectrum (Fig. 1D) of GNS/Pt/PANI nanocomposite, the related peaks to C, O and Pt were observed. The presence of Pt in EDX pattern reflects nature of Pt nanoparticles. It worth to noted that the obtained results are in good agreement with observed results from the XRD pattern (Fig. 1A). Finally, these results verified the successful synthesis of GNS/Pt/PANI nanocomposite.

3.2. Electrochemical characterization of the GNS/Pt/PANI/GCE

Fig. 2 shows the cyclic voltammograms (CVs) of the GCE, PANI/GCE, GNS/GCE, CNT/PANI/GCE, GNS/Pt/PANI/GCE, CNT/Pt/PANI/GCE, GNS/CNT/PANI/GCE and GNS/CNT/Pt/PANI/GCE in 1 mM DA with a scan rate of 100 mVs^{-1} . As can be seen the oxidation peak current of DA on GNS/Pt/PANI/GCE is larger than that on other modified electrodes. These results verify that the GNS/Pt/PANI can facilitate the electron transfer process and consequently

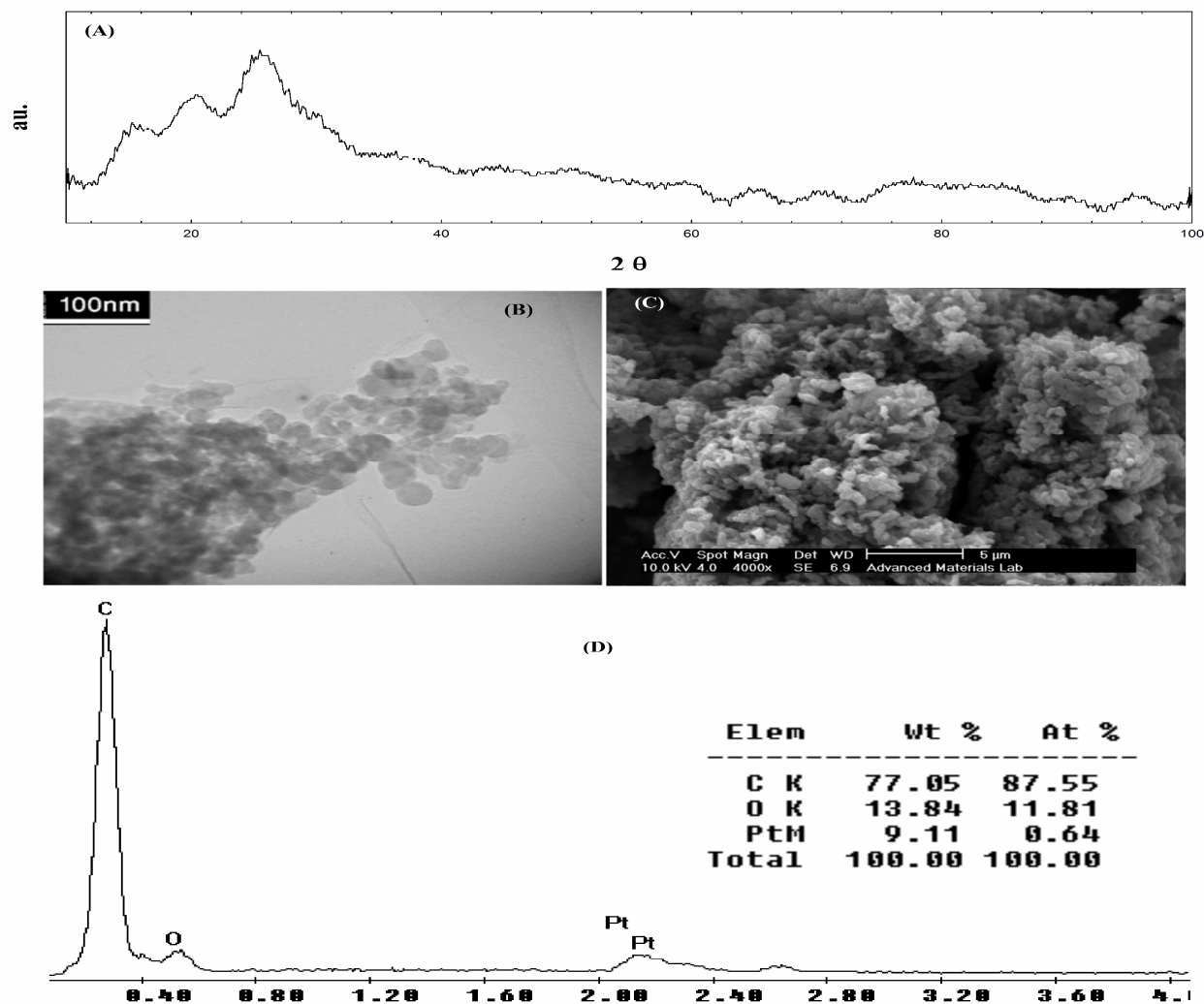


Fig. 1. (A) The XRD pattern, and the typical TEM (B) and SEM (C) images of GNS/Pt/PANI nanocomposite. (D) The EDX pattern from SEM image.

enhance the electrochemical sensitivity of the modified electrode. In this study, the dramatic increase of current response was focused and then applied for ultrasensitive determination of DA. It is evident from Fig. 2 that the onset potential for GNS/Pt/PANI/GCE compared with the other modified electrodes shows a significantly lower onset potential with a shift to a more negative potential and lower over voltage, which is attributed to a synergistic effect of GNS, Pt and PANI in the electro-oxidation and consequently ultrasensitive determination of DA.

Electrochemical response of AA in comparison to DA was shown in Figure 3 (A and B). As can be seen, a sharp wave with a high peak current for DA compare with AA was observed. Due to molecular structures of DA and AA the π - π interaction between phenyl structure of DA, and penta-heterocycle of AA, with PANI and GNS is different that led to easy arrival of DA molecules to the surface of GNS/Pt/PANI/GCE electrode [6].

3.3. Effects of the scan rate on the oxidation of DA

The effect of scan rate (ν) on the electrocatalytic activity of GNS/Pt/PANI/GCE toward oxidation of DA was investigated by CV (Fig. 4, inset). It can be seen that both the peak potentials (E_{pa}) and peak currents (I_{pa}) are dependent on the scan rate. For DA, the redox peak currents gradually increase as the scan rate increases, and a linear relation (Fig. 4) between the anodic and cathodic currents and the square root of scan rates at the range of 10–400 mV s^{-1} was observed. The linear equations according to Fig. 4 are expressed as follows:

$$I_p(\mu\text{A}) = 1.36 \nu^{1/2}(\text{mV/s}) - 35.20(\text{DA})$$

with linear relative coefficient of 0.99. The above results indicate that the oxidation of DA on GNS/Pt/PANI/GCE is a diffusion-controlled process. In addition, the electrode reactions of DA are quasireversible as the redox peaks potentials vary with the scan rates [29].

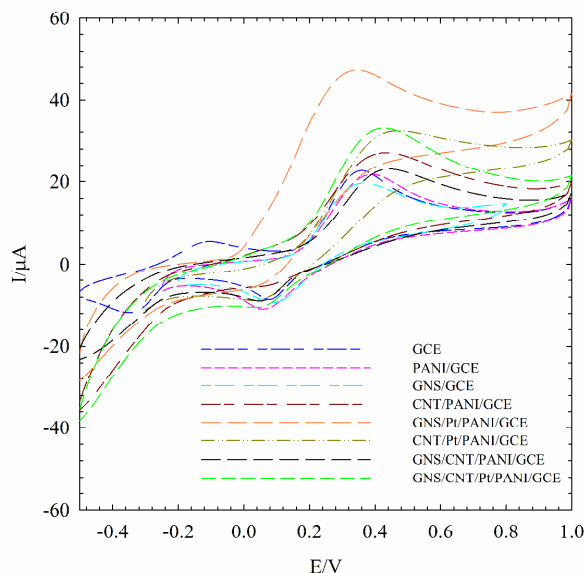
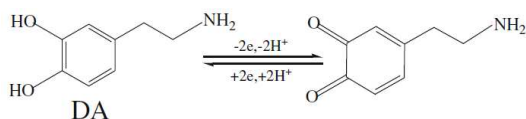


Fig. 2. Cyclic voltammograms of the GCE, PANI/GCE, GNS/GCE, CNT/PANI/GCE, GNS/Pt/PANI/GCE, CNT/Pt/PANI/GCE, GNS/CNT/PANI/GCE and GNS/CNT/Pt/PANI/GCE in 0.1 M PBS (pH 7.4) containing 1 mM DA at the scan rate of 100 mVs^{-1} .



Scheme 1. The schematic represent oxidation/reduction process of DA

3.4. Effect of pH on the oxidation of DA

The effects of solution pH on the peak potentials and peak currents of DA oxidation were studied by CV, and presented as Fig. 5A and B, respectively. As shown in Fig. 5A, the oxidation potential shifts negatively with an increase in the solution pH. A potential-pH diagram was constructed by plotting the E_p values as a function of pH (Fig. 5A). This diagram is composed of a straight line with slope as 0.061 mV/pH . Such behavior suggests that it obeys the Nernst equation for a two electron and two proton transfer reaction, as represented in scheme 1 and reported in the literature [30,31].

The oxidation peak currents of DA decreased as the pH value increased (Fig. 5B). The pH value of human blood and urine is close to 7.4, thus 0.1 M PBS solution with $\text{pH}=7.4$ was chosen for simultaneous determination of DA, because in this pH, the peak intensity for AA was lowest also.

3.5. Optimization of the electrode modification

At first, a homogeneous nanocomposite solution containing GNS, PANI and Pt was freshly prepared. In this study, GNS was used to increase the surface area and electrochemical sensitivity of the system. PANI (emeraldine salt) was used as a conducting matrix to generate the conducting nanocomposite

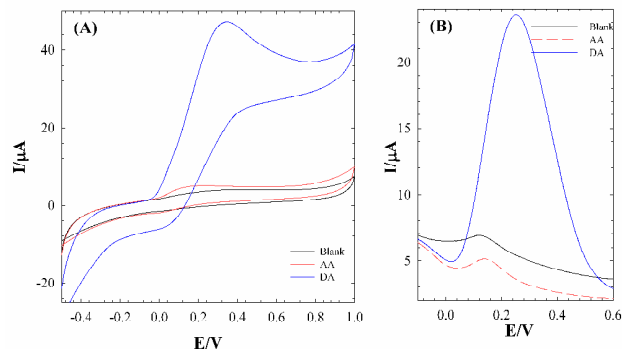


Fig. 3. Cyclic voltammograms (A) and differential pulse voltammograms (B) curves of 1 mM DA and 1 mM AA in 0.1 M PBS (pH 7.4) at GNS/Pt/PANI/GCE electrode. Blank is 0.1 M PBS (pH 7.4)

and improve the dispersibility of graphene in the nanocomposite solution. Recently, it has been reported that doping PANI with carbon based nanomaterials (e.g. CNTs or graphene) can remarkably enhance both the electrocatalytic activity and mechanical strength, leading to improved performance of these nanocomposite electrodes [32,33], and Pt is used to increase the electron transfer (ET) kinetics and electrocatalytic activity. The loading amount of GNS/Pt/PANI has a profound influence on the electrochemical response. The effects of the modifier on the electrochemical sensitivity of the GNS/Pt/PANI modified electrodes was investigated by differential pulse voltammetry using the commonly used 1.0 mM DA in 0.1 M PBS (pH 7.4). As shown in Fig. 6, the anodic peak currents increased rapidly upon increasing the loading amount of modifier from 2 to $8 \mu\text{l}$, which verifies that incorporating GNS/Pt/PANI significantly improves their electrical conductivities. However, the anodic peak currents

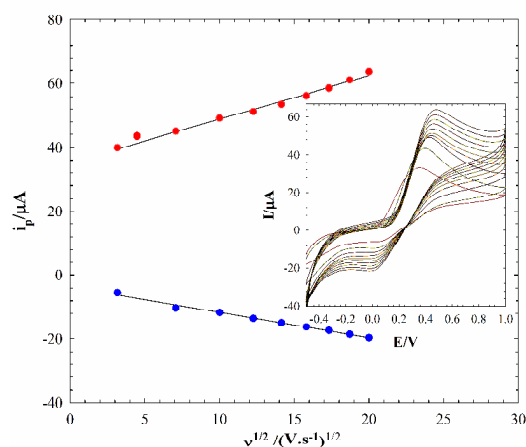


Fig. 4. Anodic and cathodic peaks current as a function of square root of scan rate measured on the GNS/Pt/PANI/GCE electrode. Inset is cyclic voltammograms of 1.0 mM DA in 0.1 M PBS (pH 7.4) at the scan rates inner to outer; 10, 20, 50, 100, 150, 200, 250, 300, 350, 400 mVs^{-1} on the GNS/Pt/PANI/GCE electrode.

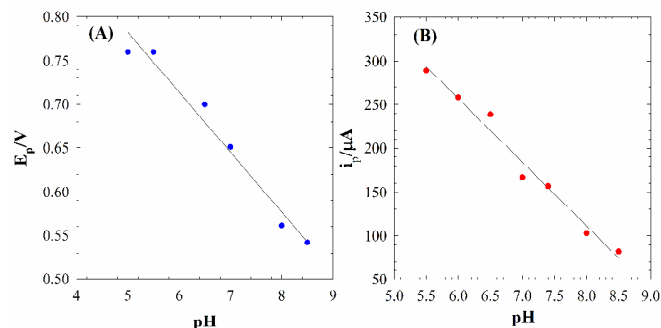


Fig. 5. Dependence of the (A) anodic peak potentials and (B) anodic currents as a function of the solution pH for 1 mM DA in 0.1 M PBS.

tend to decrease from 8 to 20 μl , which suggests a hindered mass transfer process. This decrease in current was probably caused by the agglomeration of nanocomposite on the GCE, which results in a decreases electrochemical response. Therefore, an 8 μl of modifier was chosen for subsequent studies.

3.6. Optimization of the Instrumental Parameters

The peak current of differential pulse voltammograms are also dependent to the instrumental parameters. The instrumental parameters are interrelated and can be optimized by monitoring the peak current as a function of studying parameter values, while other parameter are fixed. After a careful examination, the set of pulse amplitude (350 mV), voltage step (3 mV), voltage step time (0.3 s), and pulse time (10 ms) were found as optimized values for instrumental parameters.

3.7. Calibration and Detection Limit

The calibration curve (Fig. 7) was obtained under optimized conditions by systematically increasing the concentration of

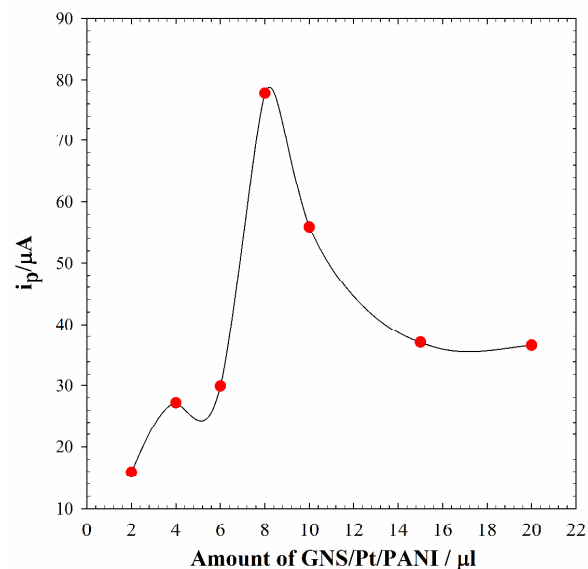


Fig. 6. Effect of the loading amount of GNS/Pt/PANI on the peak current in 1 mM DA.

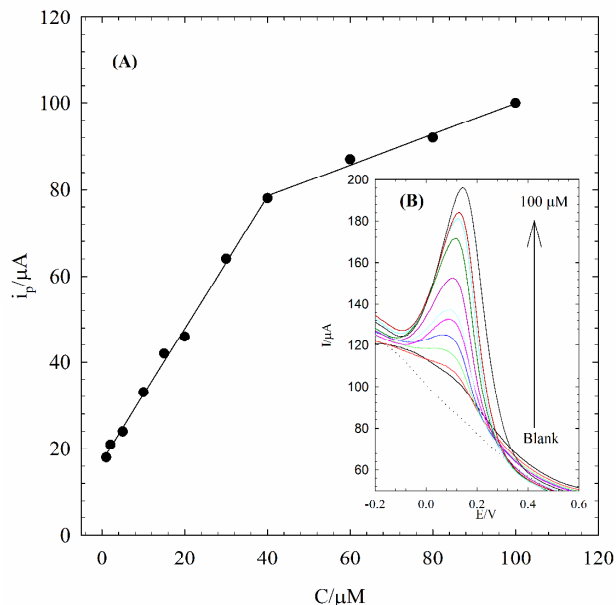


Fig. 7. (A) Calibration curve obtained from variation of the DPV anodic peak current as a function of DA concentration. (B) The differential pulse voltammograms obtained on the GNS/Pt/PANI/GCE in PBS (pH 7.4) containing different concentrations of DA; bottom to top: 0.0, 1.0×10^{-6} , 2.0×10^{-6} , 5.0×10^{-6} , 1.0×10^{-5} , 1.5×10^{-5} , 2.0×10^{-5} , 3.0×10^{-5} , 4.0×10^{-5} , 6.0×10^{-5} , 8.0×10^{-5} , 1.0×10^{-4} M DA. DPV conditions were as: voltage step (0.003 V), pulse amplitude (0.035 V), voltage step time (0.3 s) and pulse time (0.01 s).

DA from 2.0×10^{-6} to 1.0×10^{-4} M in the 0.1 M PBS (pH 7.4) and monitoring the response by DPV. In optimized experimental and instrumental conditions, two linear calibration curves from 2.0 to 40 and 40 to 100 μM DA with slopes as 1.53 and 0.35 $\mu A/\mu M$, respectively, $r^2 = 0.99$ were obtained. The detection limit (D.L.) of this electrode, was calculated from the standard deviation of the background (signal equals 3 σ of the background noise), was 0.6 μM DA, with the relative standard deviation (RSD, $n = 4$) as 0.9% for 5.0×10^{-5} M DA. The reproducibility of the GNS/Pt/PANI/GCE was evaluated by RSD, $n = 4$, of the DA with different electrodes. The RSD of 6.0% was obtained at 5.0×10^{-5} M DA. These results indicated the good and acceptable reproducibility and repeatability of the electrode.

In Table 1, the linear range and detection limit of the proposed modifier are compared with the corresponding values reported for the detection of DA by using other graphene materials. From the data given in Table 1 it is immediately obvious that the linear range and detection limit of the used nanocomposited is comparable to those reported before⁸⁻¹⁵. The linear range of our calibration curve, extended to more than two orders of magnitude, is comparable with the other references mentioned here.

Table 1. Comparison of present work and previous study that use graphene materials for determination of dopamine.

Modifier	Linear range	DL	Ref
Graphene/Polyaniline/Polystyrene	0.01nM-100 μ M	0.05 nM	[34]
Multilayer Graphene Nanoflake	1-50 mM	0.17 mM	[35]
Graphene-PVP	0.5 nM-1.13 mM	0.2 nM	[36]
Graphene Sheets/Au Nanoparticles/ Graphene Sheets	0.59-43.96 μ M	1.86 μ M	[37]
B-Cyclodextrin/Graphene	9.0 nM- 12.7 μ M	5.0 nM	[38]
Graphene Nanosheets	2-1000 μ M	0.085 μ M	[6]
Silanized Graphene	0.20-25 μ M	0.01 μ M	[29]
Graphene-Polyaniline	0.007-90 nM	0.00198 nM	[32]
Porphyrin-Functionalized Graphene	100-1000 nM	22 nM	[39]
Nitrogen Doped Graphene	0.5-170 μ M	0.25 μ M	[40]
Graphene Oxide-Templated PANI	1–14 mM	0.5 mM	[41]
Graphene/Ionic Liquids/Chitosan	0.05–240 μ M	0.05 μ M	[42]
Graphene/Pt/PANI	1-100 μ M	0.6 μ M	Present work

We define the interfering effect as the concentration of interfering species that can change the electrode response toward the DA by more than 3SA, where SA is standard deviation of the replicate DA measured signals. The interference of some common interferes on DPV response of the GNS/Pt/PANI/GCE in 5.0×10^{-5} M DA was investigated. Sucrose in 2000-fold, glucose in 400-fold, Na^+ in 20-fold, uric acid and Ca^{2+} in 8-fold, Mg^{2+} in 4-fold, glycine in 3-fold, and cystine and cysteine in equal of the DA concentration did not affect the signal obtained for DA using DPV.

4. Conclusion

In this work, combining the unique electronic properties of graphene nanosheets with the excellent properties of PANI, show excellent sensitivity and selectivity towards DA. The modified electrode can also eliminate the interference of ascorbic acid effectively. The GNS/Pt/PANI film is expected to be an ideal electrode modification material for electrochemically detection of DA. In optimized experimental and instrumental conditions, two linear calibration curves from 2.0 to 10 and from 40 to 400 μ M DA with slope as 3.60 and 0.05 $\mu\text{A}/\mu\text{M}$, respectively, $r=0.99$, and the detection limit as 0.6 μM DA was observed at pH 7.4 for GNS/Pt/PANI/GCE. Prepared sensor showed good sensitivity, repeatability, and reproducibility in this work.

Acknowledgements

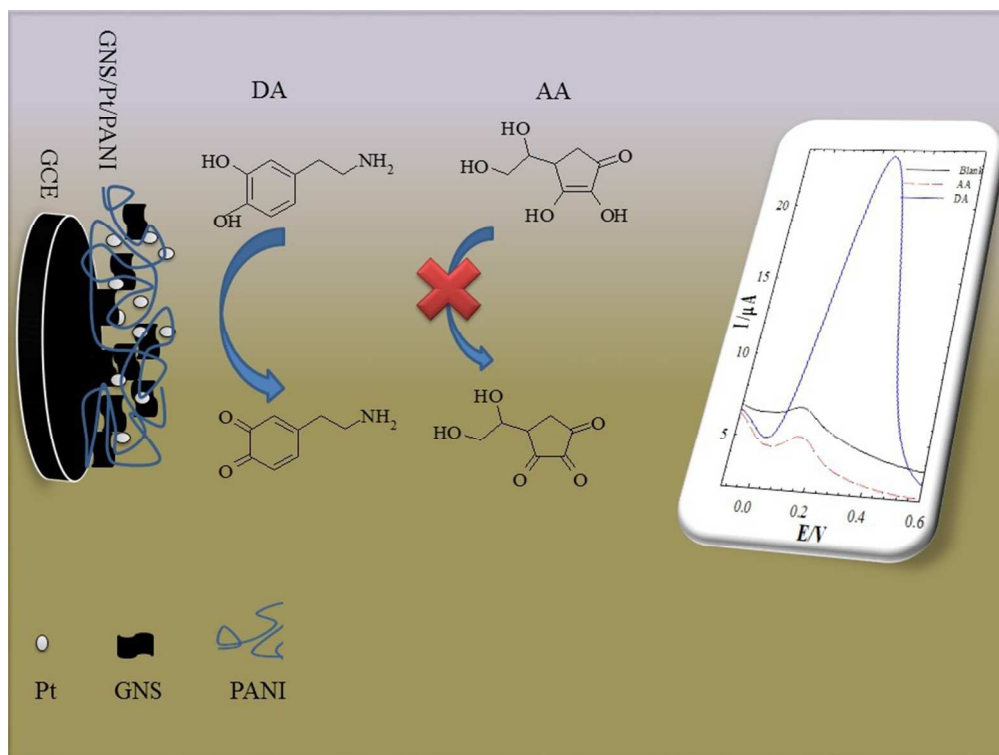
The authors gratefully acknowledge the NSTRI providing facilities for this work.

Notes and references

- [1] R. K. Shervedani, M. Bagherzadeh and S. A. Mozaffari, *Sens. Actuat. B* 2006, **115**, 614-621.
- [2] J. Y. Zhang, X. G. Chen, Z. D. Hu and X. Ma, *Anal. Chim. Acta* 2002, **471**, 203-209.

- [3] H.-X. Zhao, H. Mu, Y.-H. Bai, H. Yu and Y.-M. Hu, *J. Pharm. Anal.* 2011, **1**, 208-212.
- [4] Y.S. Zhao, S.L. Zhao, J.M. Haung, F.G. Ye, *Talanta* 2011, **85**, 2650-2654.
- [5] W. Li, D. T. Rossi and S. T. Fountain *J. Pharm. Biomed. Anal.* 2000, **24**, 325-333.
- [6] M. Bagherzadeh and M. Heydari, *Analyst* 2013, **138**, 6044-6051.
- [7] S.A. Mozaffari, T. Chang, S. M. Park, *Biosens. Bioelectron.* 2010, **26**, 74-79.
- [8] M. Bagherzadeh, S. Ansari, F. Riahi and A. Farahbakhsh, *International Journal of Electrochemistry* 2013, **2013**, 10 Pages.
- [9] H. Karimi-Maleh, F. Tahernejad-Javazmi, N. Atar, M. L. Yola, V. K. Gupta and A. A. Ensafi, *Ind. Eng. Chem. Res.* 2015, **54**, 3634-3639
- [10] M. Najafi, M. A. Khalilzadeh and H. Karimi-Maleh, *Food Chem.* 2014, **158**, 125-131.
- [11] H. Karimi-Maleh, F. Tahernejad-Javazmi, A. A. Ensafi, R. Moradi, S. Mallakpour and H. Beitollahi, *Biosens. Bioelectron.* 2014, **60**, 1-7.
- [12] H. Karimi-Maleh, P. Biparva and M. Hatami, *Biosens. Bioelectron.* 2013, **48**, 270-275.
- [13] M. Elyasi, M. A. Khalilzadeh and H. Karimi-Maleh, *Food Chem.* 2013, **141**, 4311-4317.
- [14] M. Asnaashari-Isfahani, H. Karimi-Maleh, H. Ahmar, A. A. Ensafi, A. R. Fakhari, M. A. Khalilzadeha and F. Karimi, *Anal. Methods*, 2012, **4**, 3275-3282.
- [15] M. Bagherzadeh and A. Farahbakhsh "Surface functionalization of Graphene" in "Graphene Materials: Fundamental and Emerging Applications" 2015, 25-65, USA, Wiley.
- [16] X. Kang, J. Wang, H. Wu, I. A. Aksay, J. Liu and Y. Lin, *Biosens. Bioelectron.* 2009, **25**, 901-905.
- [17] Y. Wang, Y. Li, L. Tang, J. Lu and J. Li, *Electrochem. Commun.* 2009, **11**, 889-892.
- [18] S. Stankovich, D. A. Dikin, G. H. B. Dommett, K. M. Kohlhaas, E. J. Zimney, E. A. Stach, R. D. Piner, S. T. Nguyen and R. S. Ruoff, *Nature* 2006, **442**, 282-286.
- [19] S. Ramakrishnan, K. R. Pradeep, A. Raghul, R. Senthilkumar, M. Rangarajan and N. K. Kothurkar, *Anal. Methods*, 2015, **7**, 779-786.

- 1
2
3
4 [20] J. Li, J. Yang, Z. Yang, Y. Li, S. Yu, Q. Xu and X. Hu, *Anal. Methods*, 2012, **4**, 1725-1728.
- 5 [21] S. Singh, P. R. Solanki, M. Pandey and B. Malhotra, *Sens. Actuat. B* 2006, **115**, 534-541.
- 6 [22] Y. P. Dong, Y. Zhou, Y. Ding, X. F. Chu and C. M. Wang, *Anal. Methods*, 2014, **6**, 9367-9374.
- 7 [23] I. Tiwari, K. P. Singh, M. Singh and C. E. Banks, *Anal. Methods*, 2012, **4**, 118-124.
- 8 [24] C. Dhand, M. Das, M. Datta and B. D. Malhotra, *Biosens. Bioelectron.* 2011, **26**, 2811-2821.
- 9 [25] M. U. Anu Prathap and R. Srivastava, *Sens. Actuat. B* 2013, **177**, 239-250.
- 10 [26] J. F. Smalley, K. Chalfant, S. W. Feldberg, T. M. Nahir, and E. F. Bowden, *J. Phys. Chem. B* 1999, **103**, 1676-1685.
- 11 [27] N. I. Kovtyukhova, P. J. Ollivier, B. R. Martin, T. E. Mallouk, S. A. Chizhik, E. V. Buzaneva, and A. D. Gorchinskiy, *Chem. Mater.* 1999, **11**, 771-778.
- 12 [28] C. Zhu, S. Guo, Y. Fang and S. Dong, *ACS Nano*, 2010, **4**, 2429-2437.
- 13 [29] S. Hou, M. L. Kasner, S. Su, K. Patel and R. Cuellari, *J. Phys. Chem. C* 2010, **114**, 14915-14921.
- 14 [30] Y. Yue, G. Hu, M. Zheng, Y. Guo, J. Cao and S. Shao, *Carbon* 2012, **50**, 107-114.
- 15 [31] A.J. Bard, L.R. Faulkner, *Electrochemical Methods: Fundamentals and Applications*, second ed., **2001**, Wiley, New York.
- 16 [32] S. Liu, X. Xing, J. Yu, W. Lian, J. Li, M. Cui and J. Huang, *Biosens. Bioelectron.* 2012, **36**, 186-191.
- 17 [33] M. K. Shin, Y. J. Kim, S. I. Kim, S.-K. Kim, H. Lee, G. M. Spinks and S. J. Kim, *Sens. Actuat. B* 2008, **134**, 122-126.
- 18 [34] N. Rodthongkum, N. Ruecha, R. Rangkupan, R.W. Vachet, O. Chailapakul, *Anal Chim Acta.* 2013, **804**, 84-91.
- 19 [35] N. G. Shang, P. Papakonstantinou, M. McMullan, M. Chu, A. Stamboulis, A. Potenza, S. S. Dhesi and H. Marchetto, *Adv. Func. Mater.* 2008, **18**, 3506-3514.
- 20 [36] Q. Liu, X. Zhu, Z. Huo, X. He, Y. Liang and M. Xu, *Talanta* 2012, **97**, 557-562.
- 21 [37] J. Du, R. Yue, F. Ren, Z. Yao, F. Jiang, P. Yang and Y. Du, *Gold Bulletin* 2013, **46**, 137-144.
- 22 [38] L.Tan, K.-G. Zhou, Y.-H. Zhang, H.-X. Wang, X.-D. Wang, Y.-F. Guo and H.-L. Zhang, *Electrochem. Commun.* 2010, **12**, 557-560.
- 23 [39] W.L. Feng, J. Ren and X. Qu, *Biosens. Bioelectron.* 2012, **34**, 57-62.
- 24 [40] Z.-H. Sheng, X.-Q. Zheng, J.-Y. Xu, W.-J. Bao, F.-B. Wang, and X.-H. Xia, *Biosens. Bioelectron.* 2012, **34**, 125-131.
- 25 [41] Y. Bao, J. Song, Y. Mao, D. Han, F. Yang, L. Niu and A. Ivaska, *Electroanalysis* 2011, **23**, 878-884.
- 26 [42] X. Niu, W. Yang, H. Guo, J. Ren, F. Yang and J. Gao, *Talanta* 2012, **99**, 984-988.
- 27
28
29
30
31
32
33
34
35
36
37
38
39
40
41
42
43
44
45
46
47
48
49
50
51
52
53
54
55
56
57
58
59
60



254x190mm (96 x 96 DPI)